College of Engineering

Lab 2: Tensile Testing

May 13, 2025

Michael Grady
L. Miller, G. Parkes
Lab Section: Wednesday, Group W5

Contents

List of Figures

List of Tables

Abstract

This experiment investigated the tensile properties of 1010 Steel to quantitatively evaluate its mechanical response under tensile loading. Hardness and tensile tests were employed to determine key parameters of the steel: ultimate tensile strength, fracture strength, elastic modulus, yield stress, strain to failure, and ductility. These results were compared to similar findings of Brass Alloy 260, Aluminum 6061-T6, and known values from relevant literature to determine the validity of the study's findings. Minor discrepancies were found in the tensile properties of the steel, most of which can be credited to material processing/experimental errors. Final results conclude a positive correlation between strength and hardness, confirming known material property relationships. However, no clear correlation was found between strength and ductility, likely due to the aforementioned experimental inconsistencies. Overall, this study emphasizes the importance of material selection for relevant engineering applications, including industrial and mechanical use. Close-up images were then captured of the fractured sections of each specimen and saved for relevant examination.

1 Introduction

This report aims to determine the tensile mechanical properties of 1010 Steel, specifically the strength, ductility, and hardness, and to compare them to Aluminum 6061-T6, and Brass Alloy 260 by identifying their stress versus strain behavior. Relevant tensile testing was used to determine appropriate tensile properties, such as the ultimate tensile strength (UTS), fracture strength, elastic modulus, yield stress, strain to failure, and ductility. In addition, hardness measurements were taken before and after testing to assess changes caused by hardening.

The selection of materials is highly dependent on their mechanical behavior in different engineering applications. Brass Alloy 260 benefits from high corrosion resistance and formability, making it useful for plumbing and fastening applications. It has moderate strength but high ductility, allowing it to withstand significant deformation before inevitable fracture[1;4]. Aluminum 6061-T6 has a high strength-to-weight ratio and is thus utilized in the aerospace and automotive fields. With high ultimate tensile strength, high yield stress, and moderate ductility, it excels in areas where weight reduction is necessary[2;4]. Group W5's material, 1010 Steel, is frequently used in structural applications, likely due to its strong balance of strength and ductility. As a low-carbon steel, it is more ductile than similar high-carbon steels, but is strong enough to be used appropriately in its popular applications[3;4].

Considering the given metals, strength is generally expected to be proportional to hardness, as harder materials can withstand plastic deformation more effectively. This occurs due to the hindrance of movement of dislocations within the material's microstructure[5]. The opposite is true for the relationship between ductility and strength. As the strength of material increases, ductility usually decreases, which means that higher strength materials reach their fracture point quicker while under stress rather than physically deforming. This is caused by strain hardening and dislocation hindrance, which restricts a material's ability to plastically deform, leading the material to be more prone to fracture[6]. The relationships between strength, hardness, and ductility are important to consider when applying the relevant material to its proper application. This experiment, as shown later in their respective figures, analyzed the trends between properties by comparing the stress-strain behaviors of the different metal alloys.

2 Methods

2.1 Experimental Procedure

To determine the necessary tensile properties and hardness values of the metal alloys, the experiment used a Mitutoyo HR-320MS Hardness Tester for Rockwell B Hardness measurements and an Instron #34SC-5 Universal Testing Machine for tensile testing.

Initial dimensions of the dogbone were recorded before testing. All initial widths and lengths of the dogbone were measured using calipers. The thickness of the dogbone was measured using a micrometer. See Appendix A for visual representation of relevant dimensions. For both the width and thickness of the gauge area, mean values and errors were found by taking multiple measurements to ensure accurate representation of the sample's dimensions. Initial hardness values were taken on the grip portion of the

specimen using the Rockwell B scale. The hardness tester applied a standard load to group W5's steel specimen (and the rest of the class' metals) to determine the material's resistance to indentation.

For tensile testing, the specimen was mounted to the Instron Universal Testing Machine, and an extensometer was attached to the specimen to track elongation. Testing began, and a controlled displacement rate was followed. The machine recorded the resulting load and displacement data, which was later used to generate Figure 1. After fracture, final dimensions were recorded of the resulting cross-section using a micrometer. These values were later used to calculate the percent reduction in area (%RA). Calipers were then used again to determine the final length of the dogbone, which supplied the calculation for percent elongation (%EL). Final hardness values were acquired from the hardness tester, this time within the gauge area, to determine the reaction of strain hardening. The test results were analyzed to obtain the relevant mechanical property values, as will be seen in Section 2.2: ultimate tensile strength (UTS), fracture strength, elastic modulus, yield stress, strain to failure, and ductility.

2.2 Data Analysis

Once the relevant values were extracted from the tensile tester and the extensometer, MATLAB was used to generate the stress strain curve, as shown in Figure 1. MATLAB employed the use of the following formulas to determine the necessary plots for Group W5's 1010 Steel Specimen. For the following equations, assume all variables that appear various times are considered the same as previously defined.

To begin the data analysis, the initial cross-sectional area of the gauge section was calculated using:

$$A_0 = w_0 * t_0, \tag{1}$$

where A_0 is the initial area, w_0 is the initial width, and t_0 is the initial thickness. The error was accounted for using:

$$\frac{\Delta A_0}{A_0} = \sqrt{\left(\frac{\Delta w_0}{w_0}\right)^2 + \left(\frac{\Delta t_0}{t_0}\right)^2}, \tag{2}$$

where ΔA_0 is the area uncertainty, and Δw_0 and Δt_0 are the micrometer's error. Engineering stress was then found using:

$$\sigma = \frac{Force}{A_0}, \tag{3}$$

where σ is the engineering stress and Force is an output vector of the tensile tester. The engineering stress vs strain curve was then plotted, with the strain (ϵ) being the x-axis output from the tensile tester.

The ultimate tensile strength (UTS) was determined to be the peak value on the engineering stress vs strain curve, checked with the error formula of:

$$\frac{\Delta \sigma_{UTS}}{\sigma_{UTS}} = \sqrt{\left(\frac{\Delta F_{UTS}}{F_{UTS}}\right)^2 + \left(\frac{\Delta A_0}{A_0}\right)^2}, \tag{4}$$

where $\Delta \sigma_{UTS}$ is UTS uncertainty, σ_{UTS} is the UTS, ΔF_{UTS} is the force error ($\pm .5\%$), and F_{UTS} is the force data.

True stress and true strain were then converted using the formulas:

$$\sigma_t = \sigma(1 + \epsilon), \tag{5}$$

where σ_t is true stress, and

$$\epsilon_t = ln(1 + \epsilon), \tag{6}$$

where ϵ_t is true strain.

Young's Modulus (E) was found by analyzing the stress-strain curve up to a predefined limit (175 MPA for 1010 Steel) to identify the elastic region. Within said region, the slope was calculated to determine E, with the following formula:

$$E = \frac{\Delta\sigma}{\Delta\epsilon}, \tag{7}$$

where $\Delta\sigma$ is the change in the y axis, and $\Delta\epsilon$ is the change in the x axis. The error in E was estimated using variations in different segments of the previously mentioned slope, and by averaging the maximum and minimum values.

For 1010 Steel, to determine yield stress (σ_y), the upper and lower yield points were determined from the curve, with the lower point being averaged over an area of 50 data points. The error was calculated using the standard deviation of said data points. The fracture strength was recorded as the stress at the final recorded strain value (the end of the curve), and its error was calculated using:

$$\frac{\Delta\sigma_{FS}}{\sigma_{FS}} = \sqrt{\left(\frac{\Delta F_{FS}}{F_{FS}}\right)^2 + \left(\frac{\Delta A_0}{A_0}\right)^2}, \tag{8}$$

where $\Delta\sigma_{FS}$ is the fracture strength uncertainty, σ_{FS} is fracture strength, ΔF_{FS} is the force error ($\pm.5\%$), and F_{FS} is the force data.

Fracture strain was measured as the final strain value as the specimen reached failure (final strain value on the curve). Its error was calculated using:

$$\frac{\Delta\epsilon_F}{\epsilon_F} = \sqrt{\left(\frac{\Delta l_0}{l_0}\right)^2 + \left(\frac{\Delta D}{D}\right)^2}, \tag{9}$$

where $\Delta\epsilon_F$ is the uncertainty in fracture strain, ϵ_F is the fracture strain, Δl_0 is the error in the caliper, ΔD is the strain error ($\pm.5\%$), and D is the change in length.

Percent reduction in area was calculated using:

$$RA = \frac{A_0 - A_f}{A_0} * 100, \tag{10}$$

where RA is the percent reduction in area and A_f is the final area ($A_f = t_f * w_f$). Its error was calculated using:

$$\Delta RA = \sqrt{\left(\frac{{A_f}^2}{{A_0}^4}\right)^2 \Delta A_0^2 + \left(\frac{1}{A_0^2}\right)^2 \Delta A_f^2}, \tag{11}$$

where ΔRA is uncertainty in RA and the uncertainty in final area is:

$$\frac{\Delta A_f}{A_f} = \sqrt{\left(\frac{\Delta w_f}{w_f}\right)^2 + \left(\frac{\Delta t_f}{t_f}\right)^2}. \tag{12}$$

Percent elongation was calculated using:

$$EL = \frac{l_f - l_0}{l_0} * 100, \tag{13}$$

where EL is the percentage of elongation. Its uncertainty was calculated using:

$$\Delta EL = \sqrt{\left(\frac{\Delta l_f}{l_f}\right)^2 + \left(\frac{1}{l_0} - \frac{l_f - l_0}{l_0^2}\right)^2 \Delta l_0^2}, \tag{14}$$

where ΔEL is the uncertainty in EL and $\Delta l_f = \Delta l_0$ is the error in the caliper.

3 Results and Discussion

To construct the stress-strain plots mentioned in Section 2.2 and shown in Figure 1, equations 1 and 3, as well as the strain vector output, were utilized to generate the curve. Equations 5 and 6 were then used to find true stress and strain and were plotted until σ_{UTS}. Equation 7 was used to find E along the elastic region. Yield stress was found by averaging the lower yield point over 50 data points. Fracture strain and stress were recorded as the final values of the curve. Finally, equations 10 and 13 were used to find the ductility measurements to complete Table 1. The initial and final recorded hardness values, coupled with the data from the other groups, helped graph Figure 2. Additionally, the strength coefficient (K) and strain hardening exponent (n) were determined through the analysis of true stress and strain beyond the elastic region. Figure 3's data was supplied from the ductility measurements as well as the UTS values. All error propagation was done to ensure reliability in results.

3.1 Engineering Stress-Strain vs. True Stress-Strain

The engineering and true stress-strain curves are shown in Figure 1 below. The dotted red line represents true, while the solid blue line represents the engineering. Note the upper and lower yield points, which removes the .002 offset method as an option for calculating yield. Once necking begins, the true curve stops, as necking reduces the cross-sectional area (CSA) - something that is not accounted for in equations 5 and 6 to convert engineering to true. After necking, the assumption of a uniform CSA is no longer relevant, making the true curve inaccurate for any point past the UTS, hence, the curve stops. If the true curve were continuously plotted, it would only rise as the instantaneous CSA would continue to decrease.

In the strain hardening region, the difference between the two curves will increase as plastic deformation progresses. The true stress accounts for the actual deformation of the material as its CSA changes, whereas the engineering stress assumes the original, constant CSA. Thus, the true curve offers a more accurate representation of the behavior of the steel in the strain hardening region.

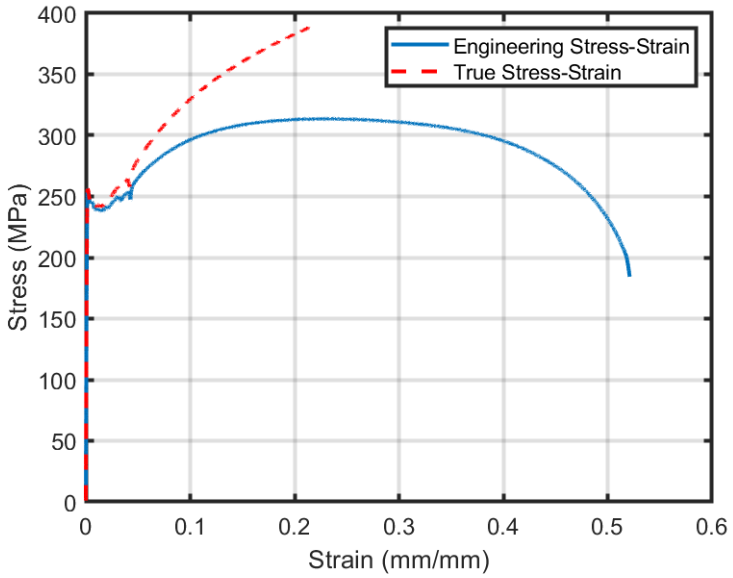

Figure 1: The engineering (blue; solid) and true (red; dotted) stress - strain plots measured of 1010 Steel

3.2 Tensile Properties

Table 1, shown below, displays the result of the aforementioned comprehensive analysis of the tensile testing data performed on MATLAB. The important tensile parameters - ultimate tensile strength, fracture strength, elastic modulus, yield stress, strain to failure, and ductility were found using the methods explained in Section 2.2. The provided values offer insight into 1010 Steel's ability to plastically deform before inevitable fracture. The resulting values of the analysis, as well as their respective errors, are listed in the table.

To determine the accuracy of the found results, the calculated mechanical properties were compared to known values as denoted in popular literature[3]. The experimental hardness values (46.75 & 73.53 HRB) differ moderately from the expected 60 HRB. The elastic modulus had a smaller difference, with the found value being 209.16 GPa compared to the expected 205 GPA. The experimental yield stress (247.29 MPa) and the experimental UTS (314.16 MPa) were both found to be significantly lower than the expected (305 MPa and 365 MPa, respectively). The found ductility values (%EL = 10.62% and %RA = 55.87%) also differ moderately from their expected (20% and 40%, respectively).

While some of the differences in value are near-significant, the trends of the data still align with the expected behavior of the 1010 Steel specimen. The deviations are likely rooted in material processing differences, previous work hardening that may have had an external effect, or experimental errors such as faulty equipment calibration. Very slight differences in initial measurements could've had a significant impact on later analysis, resulting in data deviation. Regardless, the general trend of the data follows the expected, confirming the validity of the results[7].

Table 1: Measured Tensile Properties of 1010 Steel by Group ***W5***

Property	Value	Error
Initial Hardness (HRB)	46.75	0.15
Elastic Modulus (GPa)	209.16	2.35
Yield Stress (MPa)	247.29	1.76
UTS (MPa)	314.16	1.59
FS (MPa)	188.3	0.95
Strain to failure	0.5205	0.0049
Ductility (%RA)	55.87	2.36
Ductility (%EL)	10.62	0.09
Final Hardness (HRB)	73.53	1.05

3.3 Hardness vs. Strength

To analyze the relationship between strength and hardness, Figure 2 shows the plots of yield strength and UTS vs Initial hardness for all three metals. Additionally, the change in hardness is plotted vs the strengthening exponent for the same materials.

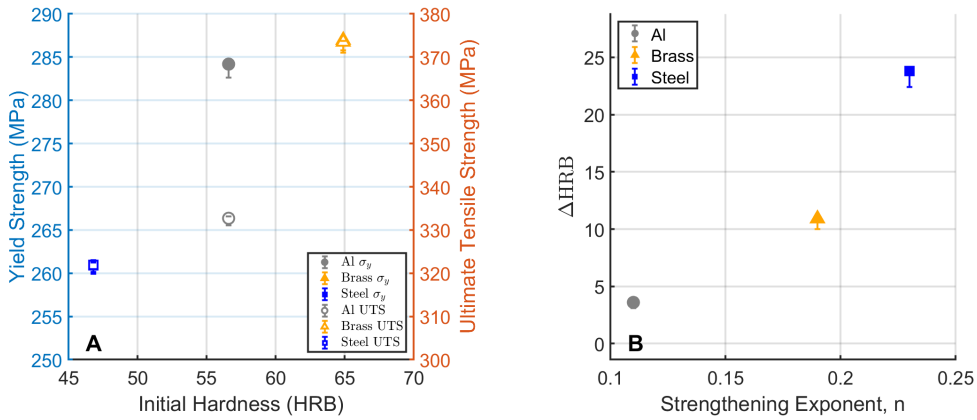

Figure 2: **A**, Rockwell B Hardness (*initially measured*) vs. yield strength (σ_y; left-axis) and ultimate tensile strength (σ_{UTS}; *right-axis*) for (Al; ●, ○), (Brass; ▲, △), and (Steel; ■, □), respectively. **B**, The change from initial to final hardness (ΔHRB) vs strengthening exponent n for Al, Brass, Steel.

The plotted data confirms our initial expectation; there is a positive correlation between hardness and strength. As evident in Figure 2A, Brass has the highest σ_{UTS} and σ_y, and the highest initial hardness value. The opposite is true for steel, with the lowest stress values and the lowest initial hardness. When looking at Figure 2B, it can be seen that steel has the highest change from initial to final hardness, and the resulting highest strengthening exponent. This follows the expectation that as materials get strained, they become harder/stronger. These findings agree with the initial assumption that harder materials will have superior strength to softer materials.

3.4 Strength vs. Ductility

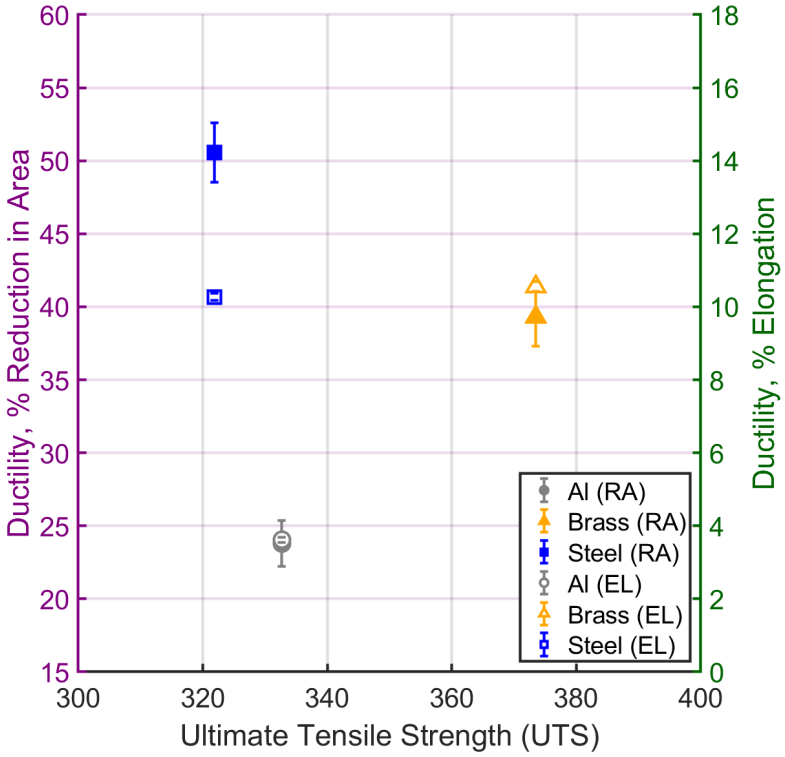

Figure 3: Ultimate tensile strength (σ_{UTS}) vs. Ductility in terms of % Reduction in Area (*%RA, left-axis*) and % Elongation (*%EL; right-axis*) for (Al; ●, ○), (Brass; ▲, △), and (Steel; ■, □), respectively.

The initial expectation for strength vs. ductility was for the relationship to be inverse - i.e. an increase in strength meant a decrease in ductility. An analysis of Figure 3 disagrees. Steel, with the lowest σ_{UTS} had a lower %EL than brass. Aluminum, who's σ_{UTS} value is between brass and steel, had the lowest %EL and %RA of the three metals. The primary relationship between ductility and strength is driven by strain hardening. Thus, the expectation was that the highest strength material, brass, would be the least ductile. The experimental values counteract this expectation, and present the claim that strength and ductility have no clear correlation. This lack of correlation likely stems from measurement uncertainty, material variability, and other reasons of deviation.

4 Conclusion

This experiment analyzed 1010 Steel's mechanical behavior while experiencing tensile loads to determine some of its key tensile parameters. Through the conduction of hardness and tensile tests, Group W5 was able to determine 1010 Steel's mechanical properties, including ultimate tensile strength, fracture strength, elastic modulus, yield stress, strain to failure, and ductility. The experimental values were compared to known values in popular literature, and were relatively similar, with most trends being similar. There were some significant deviations, like a greater than 50 MPa difference between experimental and

expected σ_{UTS} and σ_y, but most of the values followed known trends. Said deviations likely stem from material processing differences, material variability, or experimental errors such as faulty equipment calibration. A positive correlation was found between strength and hardness, but no correlation was found between strength and ductility. This variance is likely due to similar aforementioned experimental errors.

Because of the lack of correlation between strength and ductility, it is difficult to call the experiment a success. Yes, a positive relation was found between strength and hardness, and the tensile properties of 1010 Steel were close enough to expected. But, the lack of an inverse proportionality between strength and ductility results in a hypothesis that was not accepted. To ensure success in future experiments, more tests could be completed per group to accrue more data, and more care could be taken to clarify test procedures.

References

[1] "Cartridge Brass, UNS C26000 (260 Brass), OS100 Temper Flat Products." [Online]. Available: https://www.matweb.com/search/DataSheet.aspx?MatGUID=aeac472e2ef04f12bddb09ea8fab8379. [Accessed: 14-Mar-2025].

[2] "Aluminum 6061-T6; 6061-T651." [Online]. Available: https://www.matweb.com/search/DataSheet.aspx?MatGUID=b8d536e0b9b54bd7b69e4124d8f1d20a. [Accessed: 14-Mar-2025].

[3] "AISI 1010 Steel, Cold Drawn." [Online]. Available: https://www.matweb.com/search/DataSheet.aspx?MatGUID=025d4a04c2c640c9b0eaaef28318d761. [Accessed: 14-Mar-2025].

[4] OpenAI, "ChatGPT: Language Model," OpenAI, https://www.openai.com/chatgpt, Accessed: March 14, 2025, Prompt: "What are the applications of Brass Alloy 260, Aluminum 6061-T6, and Steel 1010 - and why are they used in said applications?"

[5] Zhang, P., Li, S. X., and Zhang, Z. F., 2011, "General Relationship between Strength and Hardness," Materials Science and Engineering: A, 529, pp. 62–73. https://doi.org/10.1016/j.msea.2011.08.061.

[6] Gao, Y. F., Zhang, W., Shi, P. J., Ren, W. L., and Zhong, Y. B., 2020, "A Mechanistic Interpretation of the Strength-Ductility Trade-off and Synergy in Lamellar Microstructures," Materials Today Advances, 8, p. 100103. https://doi.org/10.1016/j.mtadv.2020.100103.

[7] OpenAI, "ChatGPT: Language Model," OpenAI, https://www.openai.com/chatgpt, Accessed: March 15, 2025, Prompt: "What could have caused calculated material properties to be different from their expected values?"

A Appendix: Engineering Drawing of Tensile-Test Specimen